Ain Shams Engineering Journal 13 (2022) 101769

Contents lists available at ScienceDirect

Ain Shams Engineering Journal

journal homepage: www.sciencedirect.com

A study of micro-scale solder bump geometric shapes using minimizing energy approach for different solder materials

Ab Aziz bin Mohd Yusof [a], Mohd Al Fatihhi Mohd Szali Januddi [b], Muhamad Noor Harun [c,d,*]

[a] School of Mechanical Engineering, College of Engineering, Universiti Teknologi MARA, UiTM, Johor Branch., Malaysia
[b] Advanced Facilities Engineering Technology Research Cluster (AFET), Plant Engineering Technology (PETech) Section, Malaysian Institute of Industrial Technology, Universiti Kuala Lumpur, Malaysia
[c] School of Mechanical Engineering, Faculty of Engineering, Universiti Teknologi Malaysia, Malaysia
[d] Sport Innovation and Technology Centre (SITC), Faculty of Engineering, Universiti Teknologi, Malaysia

ARTICLE INFO

Article history:
Received 28 March 2020
Revised 8 February 2022
Accepted 8 March 2022
Available online 19 March 2022

Keywords:
Solder bump
Surface tension
Solder density
Standoff height
Maximum width

ABSTRACT

Demand for more interconnection joints between semiconductor devices can be realized with solder bump technology. Surface tension and density are usually material properties related factors that affect solder bump geometric shape. Therefore, to cope with this fast-changing microarchitecture design in semiconductor technology, a better understanding of the solder bump geometric shape is needed. This study used a static equilibrium force approach to integrate the surface tension and gravitational energy into the solder energy content. Surface Evolver software was used to perform calculations and deliver the final solder bump shape. Perfect agreement with less than 10 % comparison between previous studies and the current Surface Evolver results was found. According to statistical analysis using SPSS, the maximum width of solder shape is closely related to the surface tension.

In contrast, the maximum standoff is highly correlated with the solder density. By changing the solder volume, the solder bump changes from standard flip-chip bump to Cu pillar bump with consistency in maximum width to maximum standoff height ratio of 1.5. This study shows that the bumping technology can produce various sizes of solder bumps to meet new electronic packaging requirements.

1. Introduction

Bumping technology is highly demanding in semiconductor devices' manufacturing process to replace wire bond technology [1,2]. In addition, they are driven by a desire to produce high input/output (I/O) terminal density on the wafer by packing more desirable functions on the device using a reliability packaging process [3,4]. Simultaneously, this situation encourages various bumping technologies that would greatly benefit the semiconductor process [5].

The advantages of targeting on smaller solder bump technology are: (1) it produces a fine pitch and high-density bump that can increase the number of interconnecting per silicon die area, (2) it produces low shape profile on the assembly, (3) it increases traveling speed by reducing electron pathway through a shorter joint between terminals and (4) it involves low-cost production by reducing package substrate layer. On the other hand, the challenges faced for this type of interconnection are: (1) it causes the planarity and warpage of the thinner silicon die [6], (2) it causes surface defects, (3) it calls for low profile interconnection that requires stress compensation such as bump chasing to produce a better connection and (4) it increases the complexity of the assembly process. Apart from these, there is high demand for the small bump calls for the stacked packaging and stack chip design and silicon via in silicon packages [7].

This demanding technology depends on the shape of the solder bump and the solder material properties to determine the interconnection joint's quality and reliability [8–10]. Unfortunately, not many studies have been carried out to see the factors influencing the solder bump formation geometry at different sizes [3,11].

* Corresponding author at: School of Mechanical Engineering, Faculty of Engineering, Universiti Teknologi Malaysia, Malaysia.
E-mail address: mnoorharun@utm.my (M. Noor Harun).
Peer review under responsibility of Ain Shams University.

Production and hosting by Elsevier

https://doi.org/10.1016/j.asej.2022.101769

As a result, the solder bump prediction becomes a critical issue that needs to be considered in the solder bump development process [12].

The different geometrical shape of solder bump was used for different device designs. Solder volume, surface tension, density, and contact angle between solder and pad are the parameters related factors that determine its shapes [13–16]. Combining these factors causes the minimaxing of the solder surface area to happen and can be calculated using the minimaxing surface energy or capillary force for pressure differences on the fluid-gas boundary as discussed by Zei et al., Pfeifer and Krammer et al. [17–19]. Changing from standard solder bump to Cu pillar bump improves the ability to control solder diameter and standoff height since the interconnection shape changes from spherical to the cylindrical joint.

Based on the mentioned items, this study was carried out to investigate solder bump geometric shape-related factors and the solder's ability to form different sizes of solder bumps for different material properties. The study will focus on minimizing the surface area by minimizing the total energy of the solder. The integration of the surface tension on the area carried out on the contact line was influenced by the solder volume and contact angle to represent the actual solder bump geometric shape produced by the manufacturing process.

2. Method

2.1. Numerical method

The availability of experimental data for the solder bump is limited. Hence, predicting the solder bump formation during the reflow process was necessary. Therefore, six assumptions based on the energy approach analytical solution have been made [12]: (1) surface tension is uniform without a temperature gradient, (2) density is uniform across the geometry, (3) The final geometric shape is considered as static equilibrium force, (4) molten solder is allowed to move and wet on the pad according to the model contact angle and the applied constraints, the contact angle between the solid surface and molten solder is assumed to be constant, and (6) the material properties of density and surface tension were focused specifically at 220 ^{O}C where any changing in the mentioned properties during the reflow process was not included in the simulation.

The energy-based approach is a proven method that accurately predicts the solder bump's geometric shape [12,20,21]. The total energy, E_T consists of surface energy from the surface tension, E_S and the gravitational energy, E_G which is influenced by the weight and height of the solder relative to its base:

$$E_T = E_S + E_G \tag{1}$$

The surface tension energy, E_S is the energy that is formed due to the interfacial tension on the contact line of the solder.

$$E_S = \iint \gamma dA \tag{2}$$

The calculation of the surface tension energy is as follows:

$$E_T = y \int -\gamma cos\theta dx \tag{3}$$

Where γ is the surface tension of the molten solder, θ is the contact angle where the surface force is resolved, y is the width of the solder in constant value, and dx is the increment in the x-axis used for integration.

Under the influence of the gravitational force, the weight effect of the molten solder is configured as follows:

$$E_G = \iiint \rho gz dV \tag{4}$$

The equation is detailed as in the following in the Surface Evolver:

$$E_G = zy \int \rho g dx \tag{5}$$

Where z and y are the height and width of the solder volume, ρ is the solder's density, g is the gravitational acceleration, and dx is the increment in the x-axis used for integration which is similar to Eq. (3). The given total surface energy is based on minimaxing the contained energy:

$$min(E) = min\left[y \int -\gamma cos\theta dx + zy \int \rho g dx\right] \tag{6}$$

The volume is constrained based on the assigned value as in the following equation, where V0 is the volume assigned to the input file.

$$\iiint dv - V_0 = 0 \tag{7}$$

2.2. Simulation

Surface Evolver (Freeware, Version 2.70, USA) was used to solve the numerical formulations of Eqs. (1)–(7) and predict the solder bump's geometric shape. The force equilibrium approach is based on the surface area evolution, which works towards minimum energy content using the gradient descent method [22]. The initial input data file for Surface Evolver, containing an initial geometry database of the solder bump, geometric constraints, defined material properties (density and surface tension), and wetting conditions based on contact angle. Line integration was applied on the solder bump's contact line to replace the contact vertices' energy and volume and the edge of the solder bump faces. During reflow treatment of the solder bump formation, molten solder was wetted on the metal pad covered by solder resist. The solder resist was to prevent the molten solder from getting wet on the surrounding area. The contact angle of 110 degrees was assigned to the input file to represent the wetting condition between the metal pad and solder resist. The constraint in the z-axis is applied on the mounted solder's touching edges while allowing it to move in the y-axis and x-axis.

2.3. Validation

The validation was done by comparing the results obtained with the previous study by Ya-Yun Chou et al. [20]. The standoff and maximum width of solder bump were captured during the reflow process. The solder was assumed to melt and contain consistent material properties over its volume completely. Five models with different solder volumes were selected for comparison. Maximum width and maximum standoff were used as parameters for the validation purpose. The input information for the validation obtained from Ya-Yun Chou's et al. study is listed in Table 1 [20].

Table 1
Material properties, volume, and contact angle for Solder 63 % Sn–37 % Pb used in the study for validation purposes.

Item	Detail
Surface tension (mN/m)	498.00
Density (gm/cc)	8.90
Volume (mm^3)	0.12
Contact angle (degree)	110.00

Table 2
Material properties of the solder at the liquidus temperature of 220 ^{O}C.

Solder material	Density (gm/cc)	Surface tension (mn/m)
Sn60Pb40 [23]	8.06	475.00
Sn63 [24]	8.40	490.00
Sn90Pb10 [23]	7.16	506.00
Sn96.5Ag3.5 [23]	7.05	536.00
Sn100c [25]	7.40	542.45
SAC105 [26]	7.35	542.60
SAC305 [26]	7.40	544.90
SAC405 [26]	7.45	546.00
SAC387 [27,28]	7.44	548.00

Manual measurement of the solder bump's final geometric shape was done using the calibrated image pixel of the pad length's known size. The outmost pixel boundary was selected as the maximum point for the bump dimension. The results were compared with the past literature.

2.4. Material properties

The nine solder materials commonly used in semiconductor devices were selected for the investigation, as shown in Table 2 [23–28]. Density and surface tension were the two material prop-

Table 3
Solder bump design rule and standard specification [30].

Item	Standard flip chip bump	Fine-pitch bump	Micro-bump	Wide-pitch Cu pillar bump	Fine-pitch Cu pillar bump
Bump size (μm)	≤ 120	≤60	≤30	≥20	≥7
Bump height (μm)	≤90	≤50	≤25	≤30	≤15
Post height (μm)	5–15	5–15	5–15	≥20	≥5
Bump size tolerance	±10 %	±10 %	±10 %	±10 %	±10 %
Bump height range (within wafer)	±15 %	±15 %	±15 %	±15 %	±15 %
Bump height range (within chip)	15 %	15 %	15 %	15 %	15 %

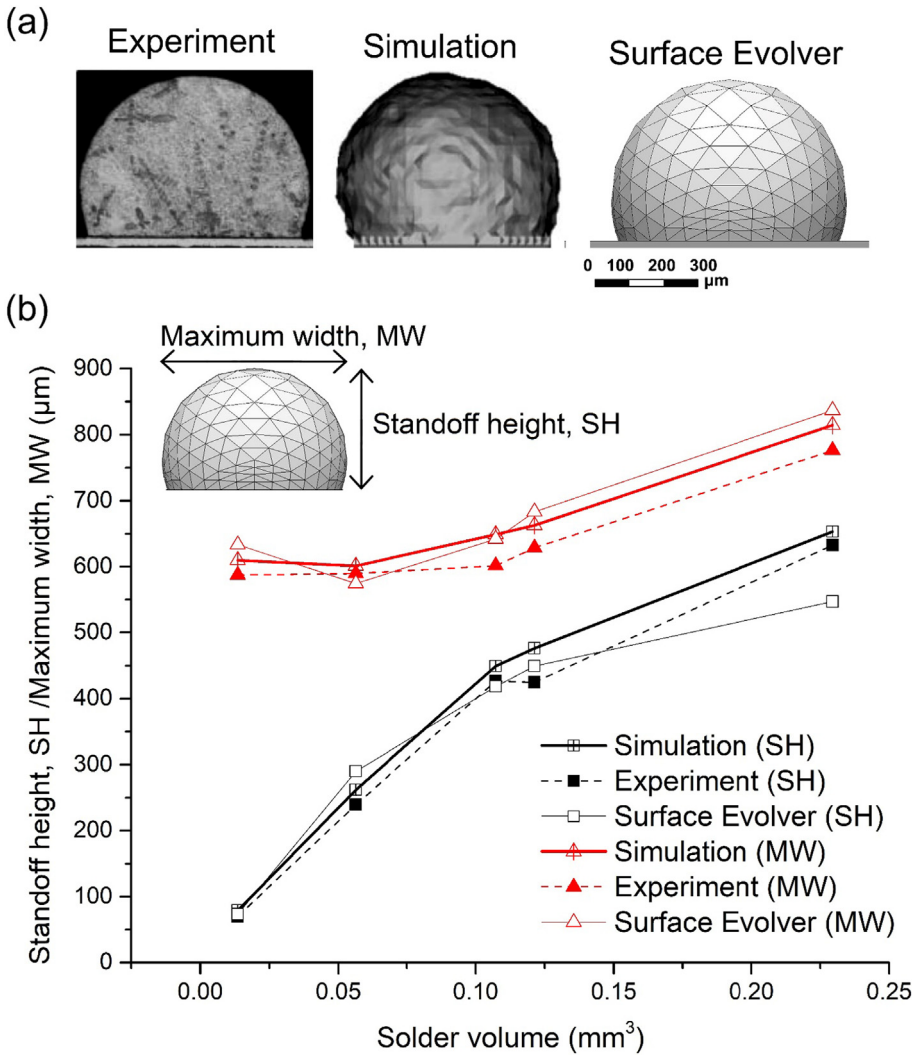

Fig. 1. Comparison of results obtained from the previous study and the current Surface Evolver.

erties used to predict the solder geometric shape. Solder density ranged from 7.44 to 8.40 gm/cc, while density ranged from 475.00 to 548.00 mN/m. The material properties of the solder were capture at 220 ^{O}C [20,23–26,29]. At this point, the solder were melted entirely and become the molted solder. In the study done by I Kaban et al. surrounding atmosphere was control at ~ 1 bar with the utilization of a niobium getter to reduce the amount of oxygen [23]. A reducing atmosphere condition such H_2 helps to suppress oxidation on the molten solder [23,29]. In this section, 0.12 mm^3 of solder volume was applied for all the models. The final geometric shape of the solder bump for each material property predicted by the Surface Evolver contained the maximum width and standoff height, then post-processing for further analysis.

Statistical analysis for post-processing data was done using the SPSS software package (IBM Crop, version 26, USA). Pearson's correlation was used to find the correlation strength between the solder material properties and the solder bump geometric shape on the interval scale. The prior alpha of p less than 0.05 was determined by referring to a statistically significant level of 5 %.

2.5. Solder bump sizes

The ability of the solder to form different solder sizes is one of the study's interests. Table 3 shows five types of solder bump and their design rule and standard specification that need to be followed during the process [30].

Based on Table 3, the solder bump's main dimensions were extracted per design rules and tolerance. Five types of solder bump were modeled, and their volumes were estimated using Solidworks modeling software (Dassault Systèmes, France). The volume of the Standard flip chip bump, Fine-pitch bump, Micro-bump, Wide-pitch Cu pillar bump, and Fine-pitch Cu pillar bump were 6.7e-4 mm^3, 9.27e-5 mm^3, 1.16e-5 mm^3, 2.09e-6 mm^3, and 2.60e-7 mm^3, respectively. These values were used as the initial solder condition of the input file to fulfill Equation (7).

3. Result

3.1. Validation

Fig. 1(a) shows solder bumps from the experimental results, software simulation, and Surface Evolver for validation. The solder volume, the maximum width, and standoff height were growing exponentially. The Surface Evolver results accurately predicted the final bump shape, which was similar to the experiment and simulation from the study by Ya-Yun Chou et al.

The average difference in the percentage of standoff height obtained using the surface Evolver was compared with the previous experiment and simulation at 9.50 % and 9.31 %. The average percentage difference of maximum width obtained using Surface Evolver compared to the previous experiment and simulation was 6.74 % and 4.54 %, respectively. Both of the average percentages obtained were less than 10 % of what is acceptable for further analysis. Therefore, it is possible to predict the solder bump formation using the present Surface Evolver program code. A solder volume of 0.12 mm^3 was selected for the investigation purpose. The maximum width ranged from 679 μm to 685 μm, with an average value of 683 μm obtained from the study. The standoff height ranged from 446 μm to 451 μm with an average value of 449 μm.

3.2. Material properties

Fig. 2 (a) shows the effect of the material properties on the geometrical shape of the solder bump. As mentioned earlier in the material properties section, the volume of the solder is kept at

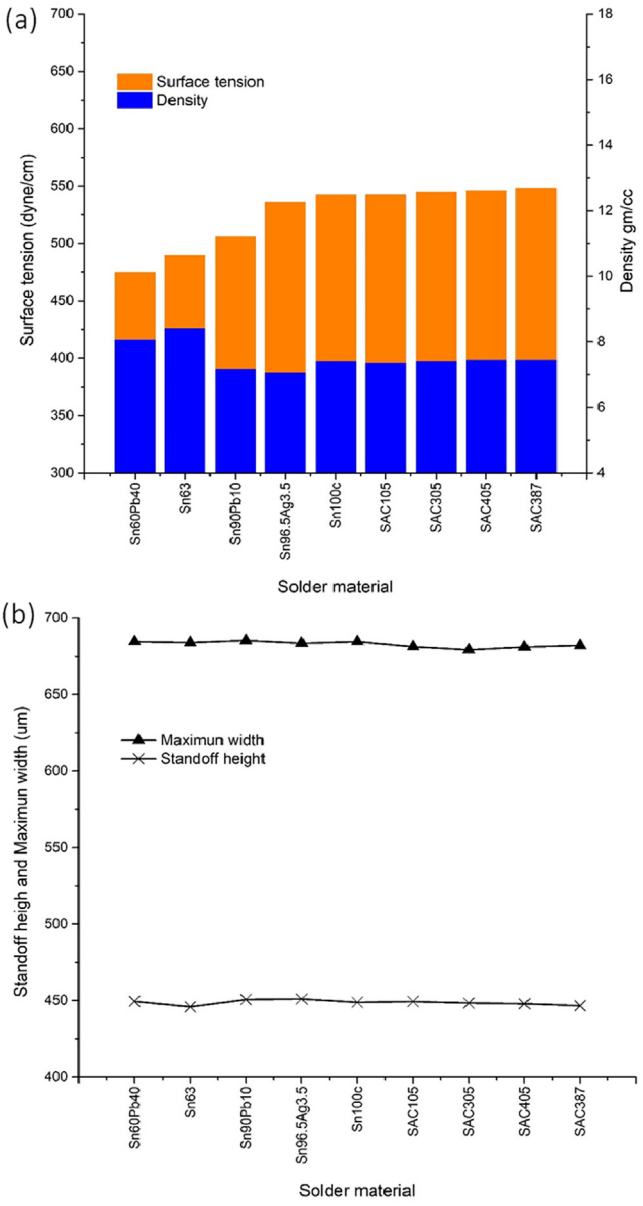

Fig. 2. (a) Material properties of the solder for solder bump. (b) Dimension of maximum width and standoff height relative to material properties of the solder.

0.12 mm^3. Therefore, every effect that happened on its shape was purely contributed by the material properties. From the list of the material properties, it is found that as the surface tension increases, density decreased. The situation happened to certain solder materials, Even though they have similar material properties. Based on the graph, it was found, increasing the surface tension possibility reduces the maximum width of the solder bump. In contrast, standoff height shows higher density material reduction and increases in standoff height in a lower density material.

The Pearson Correlation coefficient of the density and maximum width was 0.2, while the correlation between density and standoff height was −0.631. The correlation between surface tension and the maximum width was −0.643, whereas the correlation between surface tension and standoff height was −0.028. Both materials were inversely proportional to the solder bump dimension. Increasing one of the material properties would reduce the geometric shape of the solder bump.

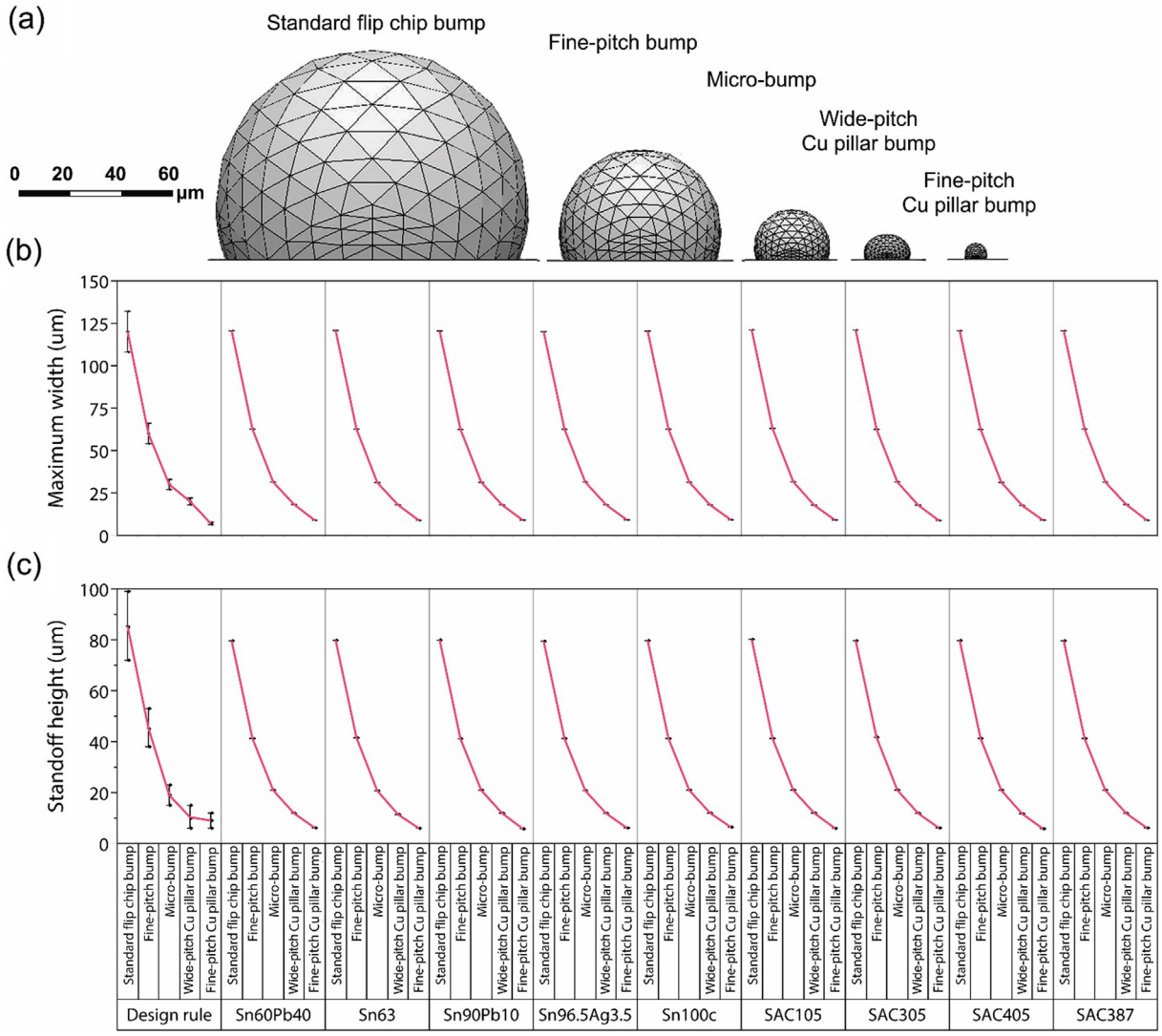

Fig. 3. The solder bump shape predicted using the Surface Evolver and its dimensions were compared to the design rules: (a) Prediction of the solder bump geometric shape, (b) Comparison of the maximum width of the solder bump from the design rule to that predicted by the Surface Evolver and (c) Comparison of the standoff height of the solder bump from design rule as predicted by the Surface Evolver.

3.3. Solder bump size

Reducing the solder volume causes a reduction in the solder bump size in both width and height while maintaining a similar shape pattern, as shown in Fig. 3(a). This semi-spherical shape was observed in many solders bump studies. It is a basic form for interconnection formation, which serves as an assembly point when the solder bump is attached to the area array device and the component deposition through the self-alignment mechanism.

The Pearson correlation coefficient between solder volume, maximum width, and standoff height was at 0.94. Increasing solder volume automatically affects the solder geometric shape, as shown in Fig. 3(a). The percentage difference between the average maximum width and the average standoff height of the design rule with the predicted geometric shape by Surface Evolver increased exponentially towards reducing solder volume. The percentage difference of maximum width and standoff height for Standard flip chip bump was 0.49 % and 6.19 %, respectively. The percentage difference of maximum width and standoff height for Fine-pitch bump was 4.41 % and 8.21 %. The maximum width and standoff height for micro bump was 4.57 % and 9.78 %. The maximum width and standoff height for Wide-pitch Cu pillar bump was 10.20 % and 17.98 %. Finally, the maximum width and standoff height for the Fine-pitch Cu pillar bump was 28.14 % and 32.90 %. The percentage differences demonstrate that a smaller solder bump is challenging to form since the smaller solder volume is hard and less flexible to achieve static equilibrium while minimizing the surface area and total energy content, as demonstrated in Fig. 3(b) and Fig. 3(c).

4. Discussion

The ability to predict, control, and manipulate molten solder as a fluid at the microscopic level is proven in this study, validated according to the previous experimental and simulation studies. This ability is an essential tool to accelerate the development of technology in the semiconductor industry. Variations in qualitative and quantitative geometric shapes occurred due to 4 main factors: (1) surface tension of the solder, (2) density of solder (3) contact angle of the surface, and (4) volume of the applied solder. Viscosity is not included in the study as it does not contribute much to the solder bump shape formation [31]. Consideration of the mentioned factors formed the solder bump shape according to what has been highlighted in the design rules.

The appropriate contact angle assigned to form the similar solder bump shape as the experimental result was 110 degrees. It is found that the average angle represents the situation where the bottom part of the solder touches the wettable metal pad and the not-wet surface of the solder resist. Based on the study done by Arenas et al., the contact angle for the pad is 30 degrees, and the contact angle for the substrate material act as solder resist is 120 degrees [32,33]. However, in this study, to investigate the solder bump shape, 110 degrees contact angle is believed to be the ideal angle to achieve the static equilibrium force to form a similar geometrical shape as the experimental result.

Reducing the energy content based on minimizing the surface area model was used to determine the solder bump's geometrical shape [18]. In this study, the shrinking in surface area of the solder bump increased with increasing volume. Meaning that higher volume produced higher surface area and resulted in a more significant reduction in its surface as it tried to achieve static equilibrium force compared to a smaller volume with a smaller surface area. The surface area reduction in the initial area to achieve static equilibrium force had increased up to 48 times higher from the micro size of the Fine-pitch Cu pillar bump to the Standard flip-chip bump. It is difficult to achieve stability with a smaller bump size as the total energy required to achieve static equilibrium force increases as the volume decreases. From the Standard flip chip to the smallest Fine-pitch Cu Pillar, the reduction in total energy per initial area required to achieve equilibrium increased up to 300 times. When the surface-to-volume ratio increases, the volume decreases, and the boundary condition needs to fulfill the contact angle. Besides, the assigned volume on the contact line of the solder becomes stiffer [18]. With a bigger volume, the solder will spread quickly to satisfy the contact angle. Since the area is bigger, it needs much area reduction with lesser energy alteration. Less volume bump experiences lesser adjustment in the area, but it is hard to satisfy the contact angle, leading to a lot of alterations in energy content [34].

As shown in Fig. 2 (a) and (b), gravity is an external force that acts on the molten solder, while surface tension is a resistance force that keeps the solder's shape by minimizing its total surface area. The higher the value of the surface tension, the lower the maximum width. While higher the density, lower the standoff height. By maintaining a similar volume but increasing the solder density causes increment in the weight of the solder. Since the solder's solidification takes around 20 s to complete, it provides ample time for the gravity force to squeeze the molten solder and flatten the top of the solder [35]. High surface tension reduces the solder shape to a minimum area which causes a reduction in maximum width. These material properties affect maximum width to standoff height at the average ratio of maximum width to standoff height of 1.5, which is higher than 1.42 of design rule and at 5.6 % difference.

In perspective to scale down solder bump to nano-size, it seems impossible to produce nano-size solder bump using the similar fabrication method for Standard flip-chip bump to Fine-pitch Cu Pillar bump. It is proved by the current Surface Evolver code and supported by the previous studies [36]. The nano-size bump causes instability in performing bumping from molten since it is hard to achieve static equilibrium force due to the drastic increment in the surface-to-volume ratio. Besides, the nano-size solder bump is almost similar to solder alloy nanoparticles which cause it hard to maintained atomic bonding between them at such a small volume [37]. Consequently, the situation leads to problematic issues in achieving static equilibrium force. Nano-Velcro technology has been suggested to be used in the assembly process of nano-size components as an alternative [38,39]. Also, Nano-Velcro technology could speed up the production time since it does not require solder printing and reflow the process as a conventional solder bump.

5. Conclusion

The applied method proves the capability to predict the solder bump geometric shape using a variety of bump sizes and material properties. The specific geometric shape is formed when the static equilibrium between weight and surface tension of the molten solder was achieved. Comparison between the design rule and solder bump found to be perfectly matched for all the bump sizes. This bumping technology has proven its flexibility in producing various solder bump sizes to meet the new semiconductor device requirements.

However, one of the research concerns is the ability of the solder to form a smaller bump as the size of the electronic component continuously scales down by reducing all its dimensions. Referring current result, solder bump technology is limited from one hundred micro sizes to less than ten micro sizes, resulting in difficulty fabricating the nanoscale solder bump as it will increase the surface-to-volume ratio.

Funding

No source of funding was used to complete this article.

Declaration of Competing Interest

The authors declare that they have no known competing financial interests or personal relationships that could have appeared to influence the work reported in this paper.

References

[1] Kang SK, Gruber P, Shih D-Y. An overview of Pb-free, flip-chip wafer-bumping technologies. JOM 2008;60(6):66–70.
[2] Lim J, Kwon D, Rieh J-S, Kim S-W, Hwang S. RF characterization and modeling of various wire bond transitions. IEEE Trans Adv Packag 2005;28(4):772–8.
[3] Park S, Bang H, Bang H, You J. Thermo-mechanical analysis of TSV and solder interconnects for different Cu pillar bump types. Microelectron Eng 2012;99:38–42.
[4] Khor CY, Abdullah MZ, Leong WC. Fluid/structure interaction analysis of the effects of solder bump shapes and input/output counts on moulded packaging. IEEE Trans Compon Packag Manuf Technol 2011;2(4):604–16.
[5] Gerber M, Beddingfield C, O'Connor S, Yoo M, Lee M, Kang D, et al. IEEE 61st electronic components and technology conference (ECTC). IEEE 2011;2011:612–8.
[6] Liu A, Wang DW, Huang H, Sun M, Lin M, Zhong C, et al. Characterization of fine-pitch solder bump joint and package warpage for low K high-pin-count flip-chip BGA. In: through Shadow Moiré and Micro Moiré techniques, 2011 IEEE 61st Electronic Components and Technology Conference (ECTC). p. 431–40.
[7] Lin Y-M, Zhan C-J, Juang J-Y, Lau JH, Chen T-H, Lo R, et al. IEEE 61st Electronic Components and Technology Conference (ECTC). IEEE 2011;2011:351–7.
[8] Ramli MII, Mohd Salleh MAA, Yasuda H, Chaiprapa J, Nogita K. The effect of Bi on the microstructure, electrical, wettability and mechanical properties of Sn-0.7Cu-0.05Ni alloys for high strength soldering. Mater Des 2020;186:108281.
[9] Wu CML, Yu DQ, Law CMT, Wang L. Properties of lead-free solder alloys with rare earth element additions. Materials Science and Engineering: R: Reports 2004;44(1):1–44.
[10] Dogan A, Arslan H. An investigation on surface tensions of Pb-free solder materials. Phil Mag 2016;96(27):2887–901.
[11] J.C. Lo, S.R. Lee, H.H. Wu, J.K. Lam, Determination of solder bump stand-off height in a flip-chip sub-mount for Micro-Opto-Electro-Mechanical System (MOEMS) packaging applications, 2008 58th Electronic Components and Technology Conference, IEEE, 2008, pp. 1887-1892.
[12] Chiang K-N, Yuan C-A. An overview of solder bump shape prediction algorithms with validations. IEEE Trans Adv Packag 2001;24(2):158–62.
[13] Dietzel M, Haferl S, Ventikos Y, Poulikakos D. Marangoni and Variable Viscosity Phenomena in Picoliter Size Solder Droplet Deposition. J Heat Transfer 2003;125(2):365–76.
[14] Sun L, Chen M-H, Zhang L, Xie L-S. Effect of addition of CuZnAl particle on the properties of Sn solder joint. J Mater Process Technol 2020;278:116507.

[15] Dogan A, Arslan H. An investigation of influencing of Sb and Bi contents on surface tensions associated with Pb-free Sn-Zn-Sb-Bi quaternary and sub-quaternary solder alloys. Phil Mag 2019;99(15):1825–48.
[16] Arslan H, Dogan A. Determination of surface tension of liquid ternary Ni–Cu–Fe and sub-binary alloys. Phil Mag 2019;99(10):1206–24.
[17] Lei Z, Ni L, Li B, Zhang K. Numerical simulation of droplet shapes in laser-MIG hybrid welding. Opt Laser Technol 2017;88:1–10.
[18] Krammer O, Illyefalvi-Vitéz Z. Investigating the self-alignment of chip components during reflow soldering. Periodica Polytechnica Electrical Engineering 2009;52(1–2):67–75.
[19] Pfeifer M. Solder bump size and shape modeling and experimental validation. IEEE Trans Compon Packag Manuf Technol Part B: 1997;20(4):452–7.
[20] Chou Y-Y, Chang H-J, Kuo J-H, Hwang W-S. The Simulation of Shape Evolution of Solder Joints during Reflow Process and Its Experimental Validation. Mater Trans 2006;47(4):1186–92.
[21] Vowell S. Microfluidics Effects of Surface Tension. Citeseer 2009.
[22] Brakke KA. The surface evolver. Experimental mathematics 1992;1(2):141–65.
[23] Kaban I, Mhiaoui S, Hoyer W, Gasser J-G. Surface tension and density of binary lead and lead-free Sn-based solders. J Phys: Condens Matter 2005;17 (50):7867–73.
[24] Bauccio M. ASM metals reference book. ASM international; 1993.
[25] Product Technical Data Sheet SN100C/SN100Ce, in: B.Z.J.J.G.C. KG (Ed.) 2003.
[26] Najib A, Abdullah M, Saad A, Samsudin Z, Ani FC. Experimental study of Self-Alignment during reflow soldering process. Journal of Advanced Manufacturing Technology 2018;12(1):2.
[27] ALPHA®Vaculoy SAC305,300,350,405,400,387,380 Lead Free Wave Solder Alloy, in: A.A. Solution (Ed.) 2018.
[28] K. Dusek, J. Urbanek, Surface tension measurement of the solders by non-wetting specimen, 2008 31st International Spring Seminar on Electronics Technology, IEEE, 2008, pp. 354-357.
[29] Moser Z, Gąsior W, Dębski A, Pstruś J. SURDAT-Database of Lead-Free Soldering Materials. Kraków: Institute of Metallurgy and Materials Science; 2007.
[30] L. SUN ELECTRONICS CO, Solder Bump, 2020. https://sun-electronics.jp/sechp/solder-bump/solder_e.html. Accessed 2020).
[31] Lai C-L, Young W-B. A model for underfill viscous flow considering the resistance induced by solder bumps. J Electron Packag 2004;126(2):186–94.
[32] Arenas MF, Acoff VL. Contact angle measurements of Sn-Ag and Sn-Cu lead-free solders on copper substrates. J Electron Mater 2004;33(12):1452–8.
[33] T. Singler, X. Zhang, K. Brakke, Computer simulation of solder bridging phenomena, (1996).
[34] Wang C, Wang C. Improved modeling for solder joint geometry and self-alignment in flip chip bonding. In: 2010 11th International Conference on Electronic Packaging Technology & High Density Packaging. p. 747–52.
[35] Ji H, Wang Q, Li M. Microstructural Evolution of Lead-Free Solder Joints in Ultrasonic-Assisted Soldering. J Electron Mater 2016;45(1):88–97.
[36] Kim I, Kang MI, Kim SW, Jung E, Lee SH. Thermal diffusivity of Sn–Ag–Cu-based, Pb-free, micro- and nano-sized solder balls. Thermochim Acta 2012;542:42–5.
[37] W. Guan, S.C. Verma, Y. Gao, C. Andersson, Q. Zhai, J. Liu, Characterization of Nanoparticles of Lead Free Solder Alloys, 2006 1st Electronic Systemintegration Technology Conference, 2006, pp. 7-12.
[38] Durán S, Novo S, Fernández-Regúlez M, Duch M, Gómez-Martínez R, San Paulo A, et al. Silicon nanovelcro to attach inorganic microdevices to biological material. In: 14th International Conference on Miniaturized Systems for Chemistry and Life Sciences. p. 503–5.
[39] Agraharam S, Deshpande N, Jackson J, Mahajan R, Manepalli R, Pang M, et al. Wakharkar, Flip-Chip Packaging Technology for Enabling 45nm Products. Intel Technology Journal 2008;12:145–56.

Ab Aziz bin Mohd Yusof received his bachelor degree in Mechanical engineering from Universiti Teknologi Malaysia, UTM (Malaysia) in 2010 and Ph.D. in Biomedical engineering in 2017 from Universiti Teknologi Malaysia (Malaysia). Currently works as a Senior lecturer in Faculty of Mechanical engineering at Universiti Teknologi Mara, UiTM. His research interests are computational simulation (FEA, CFD, FSI), manufacturing and electronic packaging.